Optics Communications 417 (2018) 83–88

Contents lists available at ScienceDirect

Optics Communications

journal homepage: www.elsevier.com/locate/optcom

Coatings influencing thermal stress in photonic crystal fiber laser

Dongqing Pang *, Yan Li, Yao Li, Minglie Hu

Ultrafast Laser Laboratory, Key Laboratory of Opto-electronic Information Technology (Ministry of Education), College of Precision Instrument and Optoelectronics Engineering, Tianjin University, 300072 Tianjin, China

ARTICLE INFO

Keywords:
Thermal stress
PCF fiber
High power fiber laser

ABSTRACT

We studied how coating materials influence the thermal stress in the fiber core for three holding methods by simulating the temperature distribution and the thermal stress distribution in the photonic-crystal fiber laser. The results show that coating materials strongly influence both the thermal stress in the fiber core and the stress differences caused by holding methods. On the basis of the results, a two-coating PCF was designed. This design reduces the stress differences caused by variant holding conditions to zero, then the stability of laser operations can be improved.

1. Introduction

Laser additive manufacturing (LAM) is becoming a new generation of fabrication technology [1]. There have already been several commercial products of LAM using high-power continuous-wave (CW) lasers or millisecond pulses lasers. However, there are still many problems, such as poor accuracy caused by large heat-affected zone and failure to fabricate high temperature materials with large conductivity. In 2015, Nie [2] demonstrated that femtosecond laser additive manufacturing can improve mechanical properties and can fabricate the materials which cannot be made by CW lasers.

Femtosecond laser additive manufacturing requires stable high power (at least 50–100 W) femtosecond pulse fiber lasers. A major and continuing challenges to high power CW fiber lasers and femtosecond pulse fiber lasers, especially femtosecond photonic-crystal fiber (PCF) lasers [3], is to reduce the thermal stress and to improve the stability of the laser operation. The thermal load in the fiber core is determined by the quantum efficiency. For example, the quantum efficiency of Er^{3+}-doped fiber laser at the wavelength 1.5 μm is less than 60% [4]. In this case, an output power of 10 W generates about 4 W thermal load in the core. Water cooling is necessary even when the laser power is only several tens Watts. So the thermal stress is also a major factor for the fiber lasers operated at some special wavelengths.

There have been many studies about the temperature distribution in double-clad fiber lasers [5,6] and PCF fiber lasers [7–10] at high thermal load. Many effects have been investigated, such as the gain competition effects [11,12], the variation of the waveguide modes [13,14], and the heat coupled laser rate equations [15], because the thermal stress is detrimental to high power fiber lasers. There have been several excellent review papers about high-power fiber lasers [16] and high power ultrafast fiber lasers [17].

In this paper, we studied how coating materials and holding methods influence the thermal stress in the fiber core by simulating the temperature distribution and the thermal stress distribution in the PCF. Our results demonstrate that coating materials have a great influence on the thermal stress in the core, and different holding methods also strongly influence the thermal stress in the core. However, choosing proper coating materials can reduce the stress and the stress sensitivity to holding methods. On the basis of the results, we designed a PCF with two coatings, a soft polymer primary coating as a stress buffer and a hard metal outer coating as a stress eliminator. This design can remove the influence of holding methods on the thermal stress, and at the same time decrease the thermal stress and provide enough protection for fibers. This design can improve the stability of the operation of high power fiber lasers.

2. Theory of thermal heat dissipation

The temperature distribution in a PCF laser can be described by the conduction heat equation

$$-\nabla \cdot [K \nabla T(x, y)] = Q(x, y) \tag{1}$$

where $T(x, y)$ is the temperature distribution, K is the thermal conductivity and $Q(x, y)$ is the heat source density. K_{silica} is 1.37 $W \cdot m^{-1} \cdot K^{-1}$, K_{air} is 2.58×10^{-2} $W \cdot m^{-1} \cdot K^{-1}$, $K_{polymer}$ is typically 0.2 $W \cdot m^{-1} \cdot K^{-1}$ [18]

* Corresponding author.
E-mail address: pangdongqing@tju.edu.cn (D. Pang).

https://doi.org/10.1016/j.optcom.2018.02.019
Received 27 November 2017; Received in revised form 28 January 2018; Accepted 7 February 2018

Table 1
Temperature-dependent coefficients for heat exchange [20].

	20 °C	40 °C	60 °C	80 °C	100 °C
C_1/air	1.38	1.34	1.31	1.29	1.27
C_1/water	105	149	179	205	227

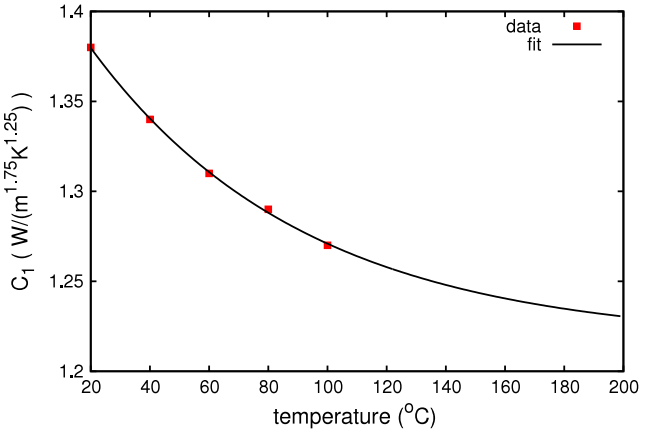

Fig. 1. Fit C_1 for air by using exp function.

and K_{copper} is 298 $W \cdot m^{-1} \cdot K^{-1}$. The heat source is

$$Q(r) = \begin{cases} \dfrac{P_{heat}}{\pi a^2} & r \le a \\ 0 & r > a \end{cases} \tag{2}$$

where a is the radius of the doping area (not the mode area) and P_{heat} is the heat load determined by the quantum efficiency of lasers. The simulation results outside the core are the same as that when considering the distribution of the heat source, i.e., P_{heat} is a function of r in the doping area due to the power distribution of the pump laser. Moreover, the constant P_{heat} is a good approximation for cladding-pumped fiber lasers. So this simple model is used in our simulation.

The heat dissipation from the coating to the ambient air usually involves convective and radiative mechanisms, so that the boundary condition can be described by two parts as follows,

$$-K\frac{\partial T}{\partial n}\Big|_{surface} = h(T - T_\infty) + \varepsilon\sigma(T^4 - T_\infty^4) \tag{3}$$

The radiative heat flow from the surface of the fiber is given by the well-known Stefan–Boltzmann law and there are $\sigma = 5.6705\times10^{-8}$ $W/(m^2\cdot K^4)$ and $\varepsilon = 0.95$ for silica. h is the heat convection coefficient and $T_\infty = 298$ K is the ambient temperature. The temperature dependent h is [19]

$$h = C_1\left(\frac{T_{surface} - T_\infty}{d}\right)^{\frac{1}{4}} \tag{4}$$

in which $C_1 = 1.38$ $W/(m^{1.75}K^{1.25})$ for air and $C_1 = 105$ $W/(m^{1.75}K^{1.25})$ for water [20]. Table 1 shows the values of C_1 at the different temperatures.

We fit C_1 for air by using the exponent function

$$C_1 = \alpha\exp(-\beta T) + \gamma \tag{5}$$

Fig. 1 shows the fitting curve for air.

For water, we fit C_1 by using the power exponent function

$$C_1 = \alpha T^\beta + \gamma \tag{6}$$

Fig. 2 shows the fitting curve for water.

3. Simulation results and discussions of temperature gradient

Fig. 3 shows the configuration of a five-missed holes PCF with single outer coating. The radius of the air hole is 3 μm. The hole-to-hole distance is 14 μm. Considering the fabrication process of dopant PCFs, the radius of the dopant area a should be smaller than the radius of the internally tangent circle of the six adjacent holes (11 μm), so a is selected as 9.6 μm. To decrease the fabrication difficulty of PCFs, the outer silica cladding of the PCF used in femtosecond fiber lasers is usually 100 μm-thickness, then the radius of the total silica part is 200 μm. The material of the outer coating is hard polymer and the thickness of the outer coating is 20 μm.

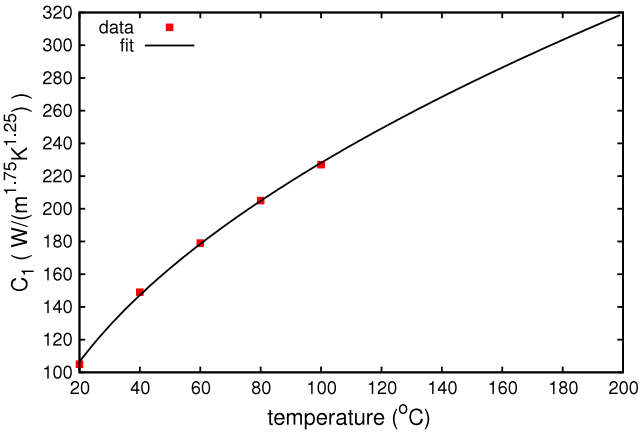

Fig. 2. Fit C_1 for water by using power exponent function.

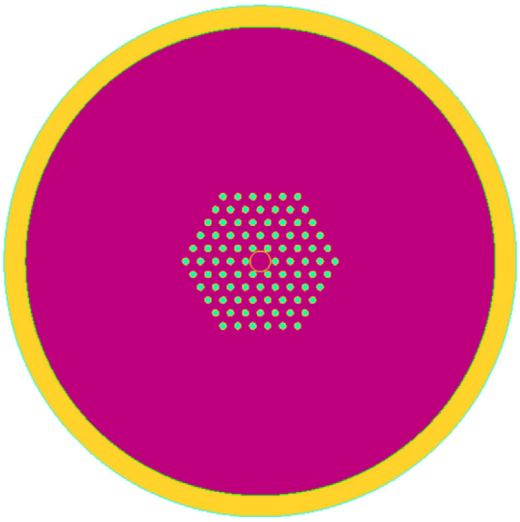

Fig. 3. A five-missed holes PCF with coating.

In simulation, we set the thermal load as 20 W/m. The core temperature is 307.3 °C and the total temperature difference $T_{core} - T_{outer}$ is 11.6 °C at 20 W/m thermal load and air cooling. Usually the fiber laser is not operated at a core temperature so high because of very low laser efficiency. Furthermore, the core temperature is much lower when using the temperature dependent parameters than that when using the constant parameters in many papers. Therefore the 20 W/m thermal load is high enough for investigation. We verified the results by varying the thermal load but they are not shown for simplicity.

The temperature distribution is nearly axial symmetric as shown in Fig. 4(a), except the temperatures at the air-hole positions. As Fig. 4(b) shows, the temperature distributions in the x- and the y-axis are a little different due to the different positions of the air holes along the x- and the y-axis. The anisotropy of holes configuration generates small anisotropy of the temperature distribution. Another notable thing is that the curve of the temperature distribution has a break point at the